Published in final edited form as:
Med Phys. 2008 March ; 35(3): 1123–1134.

Extension of the biological effective dose to the MIRD schema and possible implications in radionuclide therapy dosimetry

Sébastien Baechler[a)],
The Russell H. Morgan Department of Radiology and Radiological Sciences, School of Medicine, Johns Hopkins University, Baltimore, Maryland 21231 and University Institute of Radiation Physics (IRA-DUMSC), University of Lausanne, Lausanne, Switzerland

Robert F. Hobbs,
The Russell H. Morgan Department of Radiology and Radiological Sciences, School of Medicine, Johns Hopkins University, Baltimore, Maryland 21231

Andrew R. Prideaux,
The Russell H. Morgan Department of Radiology and Radiological Sciences, School of Medicine, Johns Hopkins University, Baltimore, Maryland 21231

Richard L. Wahl, and
The Russell H. Morgan Department of Radiology and Radiological Sciences, School of Medicine, Johns Hopkins University, Baltimore, Maryland 21231

George Sgouros
The Russell H. Morgan Department of Radiology and Radiological Sciences, School of Medicine, Johns Hopkins University, Baltimore, Maryland 21231

Abstract

In dosimetry-based treatment planning protocols, patients with rapid clearance of the radiopharmaceutical require a larger amount of initial activity than those with slow clearance to match the absorbed dose to the critical organ. As a result, the dose-rate to the critical organ is higher in patients with rapid clearance and may cause unexpected toxicity compared to patients with slow clearance. In order to account for the biological impact of different dose-rates, radiobiological modeling is beginning to be applied to the analysis of radionuclide therapy patient data. To date, the formalism used for these analyses is based on kinetics derived from activity in a single organ, the target. This does not include the influence of other source organs to the dose and dose-rate to the target organ. As a result, only self-dose irradiation in the target organ contributes to the dose-rate. In this work, the biological effective dose (BED) formalism has been extended to include the effect of multiple source organ contributions to the net dose-rate in a target organ. The generalized BED derivation has been based on the Medical Internal Radionuclide Dose Committee (MIRD) schema assuming multiple source organs following exponential effective clearance of the radionuclide. A BED-based approach to determine the largest safe dose to critical organs has also been developed. The extended BED formalism is applied to red marrow dosimetry, as well as kidney dosimetry considering the cortex and the medulla separately, since both those organs are commonly dose limiting in radionuclide therapy. The analysis shows that because the red marrow is an early responding tissue (high α/β), it is less susceptible to unexpected toxicity arising from rapid clearance of high levels of administered activity in the marrow or in the remainder of the body. In kidney dosimetry, the study demonstrates a complex interplay between clearance of activity in the cortex and the medulla, as well as the initial activity ratio and the S value ratio between the two. In some

[a)]sebastien.baechler@chuv.ch.

scenarios, projected BED based on both the cortex and the medulla is a more appropriate constraint on the administered activity than the BED based on the cortex only. Furthermore, different fractionated regimens were considered to reduce renal toxicity. The MIRD-based BED formalism is expected to be useful for patient-specific adjustments of activity and to facilitate the investigation of dose-toxicity correlations with respect to dose-rate and tissue repair mechanism.

Keywords

dosimetry; radionuclide therapy; biological effective dose

I. INTRODUCTION

The objective of dosimetry-based treatment-planning protocols in radionuclide therapy is to prescribe a clinically useful absorbed dose to the tumor while at the same time avoiding organ toxicity. If the clearance of the agent from critical organs is rapid, then the dose-rate must also be considered. Indeed, the increased dose-rate, arising from a large administered activity based on an "absorbed dose only" protocol, may cause unexpected toxicity. Even though the total absorbed dose to a dose-limiting tissue remains constant, the dose-rate can vary substantially among patients. Dose rate considerations have only recently been taken into account in radionuclide therapy dosimetry.[1–10] Those effects may be examined through the biological effective dose (BED) that relates absorbed dose and dose-rate with radiosensitivity and repair of radiation damage using the standard linear-quadratic (LQ) model.[11,12] The BED represents the dose required for a given biological effect when delivered by infinitely small doses per fraction or at very low dose-rates and is typically used to compare the response implications of total absorbed doses delivered at different dose-rates. To date, BED modeling for radionuclide therapy has accounted for the absorbed dose-rate from only a single source organ (the target).[11] This is because the formalism is based on activity kinetics in the target. In this work, the BED formalism is extended to include the effect of multiple source organ contributions to the net dose-rate in a target organ. A generalized BED formulation is developed that follows the Medical Internal Radionuclide Dose Committee (MIRD) schema.[13] The methodology is then applied to the red marrow and kidneys, which are the dose-limiting normal tissues in most radionuclide therapy. The issue of potential increased marrow toxicity due to the more rapid whole-body clearance associated with therapy using radiopeptides or engineered low molecular weight constructs as well as radioiodine therapy with protocols using recombinant human thyroid-stimulating hormone (rhTSH) is examined. The effect of cross irradiation of subkidney regions is also examined for small radiolabeled molecules. The application of BED in these examples is contrasted with its application in intact antibody mediated radioimmunotherapy.

II. MATERIALS AND METHODS

II.A. Standard BED formulation

The BED may be defined as the product of the total physical dose (D) and a modifying factor named the relative effectiveness per unit dose (RE) that quantifies dose-rate effects with respect to radiosensitivity and repair of radiation damage

$$\mathrm{BED} = D \cdot \mathrm{RE}. \tag{1}$$

It is important to note that repopulation of cells is not considered in this formulation (see Sec. IV). The model is usually applied for conventional fractionated high-dose-rate radiotherapy

with N fractions of dose d, i.e., the total dose $D = N \cdot d$. In this case, the RE function is given by

$$\mathrm{RE}=\left[1+\frac{D/N}{\alpha/\beta}\right], \tag{2}$$

where α and β are the tissue specific coefficients for radiation damage with α proportional to dose (one single event is lethal) and β proportional to dose squared (two sublethal events required for lethal damage). The α/β ratio is also named the repair capacity and quantifies the sensitivity of a given tissue to changes in fractionation. Typical values for the α/β ratio are about 5–25 Gy for early-reacting normal tissues and tumors and about 2–5 Gy for late-responding normal tissues.[14] For a single acute exposure, the fraction N is set to 1. Equation (2) assumes that acute dose fractions are spaced sufficiently to enable full recovery of sublethal damage remaining after each fraction. This is the usual situation of fractionated external beam radiation therapy (EBRT) where the regimen is based on daily fractions while the sub-lethal damage repair half-time ranges typically between 0.5 and 3 h.[15] In continuous therapy such as radionuclide therapy, the repair process of sublethal damage takes place during the radiation dose delivery and, therefore, a more general formalism is required. Assuming an exponentially decreasing dose-rate and a complete decay of the source, Dale[11] demonstrated that the RE function is given by the following expression:

$$\mathrm{RE}=1+\frac{D\cdot\lambda}{(\alpha/\beta)(\mu+\lambda)}, \tag{3}$$

where D is the absorbed dose, μ is the exponential repair rate constant that quantifies the rate of sublethal damage repair, and λ is the effective clearance rate constant given by the sum of the physical decay and the biological clearance rate constants. Note that the standard MIRD notation uses λ for the physical decay rate constant and λ_{eff} for the effective clearance rate constant.[13] In the original equation, the product $D \cdot \lambda$ is replaced by the initial dose-rate R_0. For a rapid clearance, i.e., $\lambda \gg \mu$, Eq. (3) is identical to the RE function of a single acute dose given by Eq. (2). Equation(3) is applicable only if the dose-rate, and accordingly the loss of activity in the organ, is well approximated by a monoexponential function. Howell *et al*. derived a more complex form of the RE using a dose-rate function that includes a time-dependent uptake contribution.[7] The RE function can also be expressed using the Lea–Catcheside factor G (Ref. [8]),

$$\mathrm{RE}=1+\frac{G}{(\alpha/\beta)}\cdot D. \tag{4}$$

According to Eqs. (2) and (3), G *is equal to* $1/N$ for EBRT and $\lambda/(\lambda+\mu)$ for radionuclide therapy. The factor G ranges between 0 and 1 and expresses the reduction in cell kill due to sublethal damage repair during continuous irradiation and/or between fractions. Including the factor G, the standard LQ equation may be expressed as $\exp(-\alpha D - G\beta D^2)$. The generalized Lea–Catcheside factor G for a time-dependent dose-rate $\dot{D}(t)$ is given as follows:[16,17]

$$G(T)=\frac{2}{D^2}\cdot\int_0^T \dot{D}(t)dt\int_0^t \dot{D}(w)\cdot e^{-\mu(t-w)}dw. \tag{5}$$

The second integration over the time parameter, *w*, refers to the exponential repair of first sublethal damage. The first integral term expresses the second event that can combine with the first event remaining after repair to produce a lethal lesion. As opposed to a single lethal event, sublethal damage is dependent on the rate of dose delivery. For a complete decay of the source, i.e., the radionuclide, the overall time of the treatment T goes to infinity.

II.B. BED formulation for multiple decaying sources

Assuming a temporal variation of activity in the source region *h* described by an instantaneous uptake and a multi-exponential clearance, the dose-rate to the target organ due to the single source organ *h* is given by the following functional form:

$$\dot{D}_h(t)=\dot{D}_{0,h}\sum_i^n a_{i,h}\cdot e^{-\lambda_{i,h}t} \quad \text{with} \quad \sum_i^n a_{i,h}=1, \tag{6}$$

where $\dot{D}_{0,h}$ is the initial dose-rate contribution from the source organ *h* to the target organ, *i* is multiexponential component index (i =1, …,n), $\lambda_{i,h}$ is the effective clearance rate, and $a_{i,h}$ is the dose-rate fraction coefficient. For instance, an adequate description of blood clearance requires typically a biexponential function (n =2) or a triexponential function (n =3) in case of radiopeptides. In the case of multiple source organs, each source imparts a radiation dose-rate to the target organ with a multiexponential clearance pattern related to the time-activity function. The total dose-rate to the target organ exposed to *s* source organs is then given by the sum of the dose-rates,

$$\dot{D}(t)=\sum_h^s \dot{D}_h(t)=\sum_h^s\sum_i^n \dot{D}_{0,h}\cdot a_{i,h}\cdot e^{-\lambda_{i,h}t}. \tag{7}$$

The general expression for RE assuming a time-dependent dose-rate $\dot{D}(t)$ is given by Eq. (4) with the generalized Lea–Catcheside time factor G defined in Eq. (5). Substituting Eq. (7) in Eq. (5) and solving the double integration for a complete decay of the source gives the following expression:

$$G_{s,n}=\frac{2}{D^2}\cdot\sum_{m,h}^s\sum_{k,i}^n\frac{\dot{D}_{0,m}\dot{D}_{0,h}\cdot a_{k,m}\cdot a_{i,h}}{(\lambda_{k,m}+\lambda_{i,h})(\mu+\lambda_{k,m})}. \tag{8}$$

Using the MIRD schema, the extrapolated “initial dose-rate” $\dot{D}_{0,h}$ may be expressed by the following equation:

$$\dot{D}_{0,h}=A_0\cdot S_h\cdot f_h, \tag{9}$$

where A_0 is the administered activity, S_h is the S value from the source organ *h* to the target organ, and f_h is the “initial activity fraction” obtained by extrapolating to zero time an exponential expression fitted to the activity versus time curve. In clinical dosimetry, f_h values are obtained during the biokinetic analysis based on a multiexponential fit of activity-time curve according to the function,

$$A_h(t)=A_0\sum_i^n f_h a_{i,h} e^{-\lambda_{i,h}t}, \tag{10}$$

where $A_h(t)$ is the activity in the organ h at time t. Substituting Eq. (9) in Eq. (8) gives the following expression:

$$G_{s,n}=\frac{2\cdot A_0^2}{D^2}\cdot\sum_{m,h}^{s}\sum_{k,i}^{n}\frac{f_m\cdot f_h\cdot S_m\cdot S_h\cdot a_{k,m}\cdot a_{i,h}}{(\lambda_{k,m}+\lambda_{i,h})(\mu+\lambda_{k,m})}. \tag{11}$$

In Eq. (11), the factor $G_{s,n}$ is a function of both the total dose D and the administered activity A_0. The total dose may be eliminated from the expression by inserting Eq. (9) into Eq. (7) and taking the time integral between zero and infinity; the following relation is obtained:

$$D=\sum_h^s D_h=A_0\sum_h^s\sum_i^n\frac{a_{i,h}f_h S_h}{\lambda_{i,h}}. \tag{12}$$

Substituting Eq. (12) in Eq. (11), the MIRD-based Lea–Catcheside factor is finally given by

$$G_{s,n}=\frac{2\cdot\sum_{m,h}^{s}\sum_{k,i}^{n}\frac{f_m\cdot f_h\cdot S_m\cdot S_h\cdot a_{k,m}\cdot a_{i,h}}{(\lambda_{k,m}+\lambda_{i,h})(\mu+\lambda_{k,m})}}{\left(\sum_h^s\sum_i^n\frac{a_{i,h}f_h S_h}{\lambda_{i,h}}\right)^2}. \tag{13}$$

As a test of the consistency, Eq. (13) is determined for a unique source with monoexponential clearance, i.e., $s=n=1$. In this special case, $G_{1,1}=\lambda/(\lambda+\mu)$ and the resulting RE function is identical to Eq. (3). As an example of using Eq. (13), the factor G for a unique biexponential decaying source is determined as follows:

$$G_{1,2}=\frac{\frac{a_1^2}{\lambda_1(\mu+\lambda_1)}+\frac{2\cdot a_1\cdot a_2}{(\lambda_1+\lambda_2)(\mu+\lambda_1)}+\frac{2\cdot a_2\cdot a_1}{(\lambda_2+\lambda_1)(\mu+\lambda_2)}+\frac{a_2^2}{\lambda_2(\mu+\lambda_2)}}{\left(\frac{a_1}{\lambda_1}+\frac{a_2}{\lambda_2}\right)^2}. \tag{14}$$

II.C. BED formulation for two source organs

The special case with activities located in two source organs following monoexponential effective clearance is considered, i.e., $s=2$ and $n=1$. According to Eq. (12), the total absorbed dose to the target organ is described as follows:

$$D=A_0\cdot\frac{f_1 S_1}{\lambda_1}+A_0\frac{f_2 S_2}{\lambda_2}. \tag{15}$$

In many situations, the first term corresponds to the self-absorbed dose in the target organ and the second term corresponds to the absorbed dose from activity in another organ or tissue. In this particular case of monoexponential clearance, the conventional MIRD formalism refers to

the ratio f/λ as the residence time τ. Using Eq. (13), the factor $G_{2,1}$ is expressed as a function of μ, f_1, f_2, λ_1, λ_2, S_1, and S_2,

$$G_{2,1}=\frac{\left\{\frac{f_1^2S_1^2}{\lambda_1(\lambda_1+\mu)}+\frac{2f_1f_2S_1S_2}{(\lambda_1+\lambda_2)(\lambda_1+\mu)}+\frac{2f_1f_2S_1S_2}{(\lambda_2+\lambda_1)(\lambda_2+\mu)}+\frac{f_2^2S_2^2}{\lambda_2(\lambda_2+\mu)}\right\}}{\left(\frac{f_1\cdot S_1}{\lambda_1}+\frac{f_2S_2}{\lambda_2}\right)^2}. \tag{16}$$

Unlike the absorbed dose that needs only the knowledge of residence times τ, the factor G, requires the knowledge of both parameters f and λ independently. In this special case, the function G is driven by both ratios f_1/f_2 and S_1/S_2. As mentioned before, G is smaller than 1. In Eq. (16), each of the four terms in the numerator may be interpreted as a possible combination of generating two sublethal events to cause lethal damage. The variation of RE in case of two source organs will be discussed via the use of $G_{2,1}$ for red marrow and kidneys in the next section.

II.D. BED formulation for fractionated radionuclide therapy

For treatments with a dose fractionated in multiple cycles, the BED is linearly additive[16,18] and the following expression for the total BED may be derived using Eqs. (1) and (4):

$$\mathrm{BED}=\sum_i^N D_i\cdot\left(1+\frac{G_i}{\alpha/\beta}\cdot D_i\right), \tag{17}$$

where D_i is the dose and G_i is the generalized Lea–Catcheside factor for the cycle i. For a total absorbed dose D given in N equal fractions, with a time lapse long enough to assume a complete decay of the radionuclide and full repair of sublethal damage between each cycle, Eq. (17) may be expressed as follows:

$$\mathrm{BED}=D\left(1+\frac{G_{s,n}/N}{\alpha/\beta}\cdot D\right). \tag{18}$$

It was assumed that all biokinetic parameters remain constant during the overall treatment to consider the same factor $G_{s,n}$ for each cycle. Note that Eq. (13) is independent of the fractionation scheme and thus $G_{s,n}$ may be evaluated with cumulated initial activity fractions f_h.

II.E. BED-based treatment planning

The conventional dosimetry-based approach in radionuclide therapy consists in determining the activity that would deliver the “largest safe absorbed dose” to the organ at risk. Considering a BED approach, the maximum safe absorbed dose D must satisfy the following equation:

$$\mathrm{BED}=D\cdot\mathrm{RE}=D+\frac{G}{(\alpha/\beta)}\cdot D^2, \tag{19}$$

where the BED is derived from clinical experience in EBRT. Indeed, limiting absorbed doses, such as $D_{5,5}$ that results in a 5% probability of developing severe late damage within 5 years, are available for most normal tissues in EBRT and may be converted to $\mathrm{BED}_{5,5}$ using Eq. (2)

with an appropriate dose per fraction (typically 2 Gy). The physical solution of Eq. (19) is given by

$$D=\frac{\alpha/\beta}{2G_{s,n}}\cdot\left(\sqrt{1+\frac{4\cdot G_{s,n}\cdot \mathrm{BED}}{\alpha/\beta}}-1\right), \tag{20}$$

where $G_{s,n}$ is determined using Eq. (13) with patient-specific biokinetic parameters and S values associated to the dose-limiting organ. Considering a fractionated regimen (N equal fractions), $G_{s,n}$ is replaced by $G_{s,n}/N$ in Eq. (20). Finally, the corresponding activity to be administered is easily calculated using Eq. (12).

III. RESULTS

III.A. Application to red marrow

For most nonmyeloablative radionuclide therapy, red marrow is the first dose-limiting organ. Since poor correlations between absorbed doses to red marrow and hematological toxicities have been reported in literature, it appears judicious to assess the use of BED for this purpose. The standard calculation of mean absorbed dose to red marrow is generally described as the sum of the self-absorbed dose in red marrow and the absorbed dose from activity in the remainder of the body

$$D_{\mathrm{RM}}=A_0(\tau_{\mathrm{RM}}\cdot S_{\mathrm{RM}\leftarrow\mathrm{RM}}+\tau_{\mathrm{RB}}\cdot S_{\mathrm{RM}\leftarrow\mathrm{RB}}). \tag{21}$$

$S_{\mathrm{RM}\leftarrow\mathrm{RB}}$ values are determined using the following expression:

$$S_{\mathrm{RM}\leftarrow\mathrm{RB}}=S_{\mathrm{RM}\leftarrow\mathrm{TB}}\cdot\frac{m_{\mathrm{TB}}}{m_{\mathrm{TB}}-m_{\mathrm{RB}}}-S_{\mathrm{RM}\leftarrow\mathrm{RM}}\cdot\frac{m_{\mathrm{RM}}}{m_{\mathrm{TB}}-m_{\mathrm{RB}}}. \tag{22}$$

$S_{\mathrm{RM}\leftarrow\mathrm{RM}}$ and $S_{\mathrm{RM}\leftarrow\mathrm{TB}}$ values are available from OLINDA/EXM.[19] For the reference man, the following masses are used: m_{RM}=1.12 kg, m_{TB}=73.7 kg, and m_{blood}=5.2 kg. S values for different radionuclides of interest are given in Table I. Supposing a monoexponential effective clearance, the residence times in the red marrow τ_{RM} and the remainder of the body τ_{RB} are expressed as $f_{\mathrm{RM}}/\lambda_{\mathrm{RM}}$ and $f_{\mathrm{RB}}/\lambda_{\mathrm{RB}}$. It is assumed that ($f_{\mathrm{RM}}$+ f_{RB}) corresponds to the initial activity in the whole body. In practice, f_{RM} and f_{RB} are extrapolated to the time of administration according to the best exponential fit and there is no explicit relationship between both parameters. Considering the blood-based approach,[20] the extrapolated fraction in the red marrow may be expressed as

$$f_{\mathrm{RM}}=f_{\mathrm{blood}}\cdot\frac{m_{\mathrm{RM}}}{m_{\mathrm{blood}}}\cdot\mathrm{RMBLR}, \tag{23}$$

where RMBLR is the red marrow-to-blood activity concentration ratio that ranges between 0.19 and 0.63, up to 1.0 for fragments.[21] Assuming a RMBLR of 0.5, f_{RM} is about $0.1\cdot f_{\mathrm{blood}}$. According to this method, the effective clearance half-time in red marrow is equal to the effective clearance half-time in blood.

RE functions for the red marrow are then determined using Eq. (4) with $G_{2,1}$ given in Eq. (16) (source 1=RM; source 2=RB). For the α/β ratios of red marrow cells, Fowler *et al.*[12] indicate a range of 7–26 Gy. Dale[11] assumed a value of 15 Gy for his calculations and Wilder *et al.*[10] used 10 Gy in their study. Concerning the repair half-time, Dale[11] and Howell[7] assume 1.5 h while Wilder used 0.5 h.[10] For the present study, an α/β of 10 Gy and a repair half-time T_μ of 1.5 h (corresponding to a repair rate μ of 0.46 h^{-1}) are assumed. A safety threshold of 2 Gy for absorbed dose to red marrow is generally recommended to reduce the probability of severe marrow depression.[22] Since G is smaller than 1 in any case, the highest value for RE is 1.20 according to Eq. (4). Figure 1 shows the RE isocurves of the red marrow for ^{90}Y, ^{111}In, ^{131}I, and ^{177}Lu as a function of effective clearance half-times $T_{1/2,blood}$ and $T_{1/2,RB}$, assuming an extrapolated initial intake ratio f_{RM}/f_{RB} of 0.05. This ratio corresponds to a realistic extrapolated initial intake for blood of 0.5. Since effective clearance half-times are more intuitive than effective clearance rates, λ_{blood} and λ_{RB} have been replaced by $\ln(2)/T_{1/2,blood}$ and $\ln(2)/T_{1/2,RB}$. In Fig. 2, RE functions for ^{90}Y are plotted for a different α/β of 15 Gy and then a different repair half-time T_μ of 0.5 h.

III.B. Application to kidney dosimetry

Radiation dose to kidneys is of clinical significance for peptide receptor radionuclide therapy (PRRT) because of the high tubular uptake of the peptides after glomerular filtration and retention of the radionuclides in the proximal tubular cells. Large amounts of radiolabeled peptides, such as somatostatin analogs (e.g., ^{111}In-DTPA-octreotide, ^{90}Y-DOTATOC, and ^{177}Lu-DOTATATE), retained in the renal cortex cause high radiation doses that may result in nephropathy.[23,24] Animal studies indicated that the activity distribution in the cortex and medulla depends on the antibody or peptide size.[25] According to the multiregion model of the MIRD Pamphlet No. 19 for kidneys,[26] the mean dose to tissues of the renal cortex is given by

$$D_{cort}=A_0(\tau_{cort}\cdot S_{cort\leftarrow cort}+\tau_{med}\cdot S_{cort\leftarrow med}). \quad (24)$$

The renal pelvis and medullary papillae that represent a volume of 4.2% and 0.8%, respectively, of the total kidney tissue are neglected for the present study. $S_{cort\leftarrow cort}$ and $S_{cort\leftarrow med}$ values are available from MIRD19 (Ref. [26]) and are given in Table II for the adult phantom. Since a monoexponential clearance is assumed for both subregions of the kidney, residence times τ_{cort} and τ_{med} are expressed as f_{cort}/λ_{cort}, and f_{med}/λ_{med}. Note that f is the extrapolated initial fraction of activity within the subregion and not the fractional residence time as expressed in MIRD19. It is assumed that (f_{cort} + f_{med}) corresponds to the extrapolated initial fraction of activity in the whole kidney.

To evaluate the RE functions for the renal cortex using Eqs. (4) and (16) (source 1=cortex; source 2=medulla), the following parameters proposed by Barone *et al.*[1] are used: repair half-time T_μ of 2.8 h, α/β ratio of 2.6 Gy, and maximal absorbed dose to kidneys D of 27 Gy. In fractionated EBRT, it is recommended that a kidney absorbed dose of 23 Gy (=$D_{5,5}$) should not be exceeded.[27] A higher critical dose has been tolerated for radionuclide therapy since much lower dose-rates are involved.[8] In the present study, the limiting dose of 27 Gy is applied to the renal cortex, which is most likely to be responsible for observed radiation-induced toxicity, such as nephropathy, after radionuclide therapy. Using Eq. (4), the maximal RE is 11.4. This nonrealistic case would correspond to a single acute dose delivery (G =1) of 27 Gy. In other words, 27 Gy delivered as a single acute exposure would have a devastating biological effect equal to 308 Gy delivered in very small fractions over a very long time. Figure 3 provides the RE isocurves of the renal cortex for different radionuclides of interest, as a function of ($T_{1/2,cort}$, $T_{1/2,med}$) assuming that the initial intake of radioactivity is distributed equally in the cortex and the medulla (f_{med}/f_{cort} =1). For conceivable effective clearance half-times, the RE

ranges typically between 1.4 (shown as the region to the right of the 1.6 isodose curve) and 4.0, corresponding to a BED between 37.8 and 108 Gy. In Fig. 4, RE isocurves are shown for ^{90}Y considering two different initial intake scenarios: (a) and (c) f_{cort}/f_{med}=3; (b) and (d) f_{cort}/f_{med}=1/3. In Figs. 4(c) and 4(d), RE isocurves are given taking into account fractionation effects using Eq. (18) for a two-cycle (N =2), and respectively, four-cycle (N =4), regimen. The range of RE values is then reduced to between 1.2 and 2.6, and between 1.1 and 1.8, respectively. Figure 5 shows the largest safe isodose, calculated with Eq. (20) and the $G_{2,1}$ of the cortex, as a function of $T_{1/2,cort}$ and $T_{1/2,med}$ that corresponds to a $BED_{5,5}$ of 41 Gy. The BED has been converted from the EBRT dose limit of 23 Gy using Eq. (2) with fractionation of 2 Gy. A ratio f_{cort}/f_{med} of 1 was assumed. As an example, for both $T_{1/2,cort}$ and $T_{1/2,med}$ of 40 h, the largest safe absorbed dose to the renal cortex is of about 25 Gy with a single cycle [Fig. 5(a)]and 32 Gy with a three-dose fractionation regimen [Fig. 5(b)]. The corresponding activity to be administered A_0 may be then calculated using Eq. (24). For this purpose, the total initial activity fraction in both kidneys, i.e., (f_{cort} + f_{med}), is required in addition to the ratio f_{cort}/f_{med}. Thus, assuming an initial uptake fraction of 10% in kidneys, a cumulated administered activity A_0 of 12 GBq is required to deliver an absorbed dose to the cortex D_{cort} of 25 Gy, and 15 GBq for a D_{cort} of 32 Gy. For a smaller uptake fraction of 5%, maximal tolerable activities are exactly twice as high.

IV. DISCUSSION

Figures 1–4 show that RE factors increase as effective clearance half-times decrease. Indeed, for short half-times, a higher activity has to be administered in order to reach the targeted absorbed dose. Consequently, the dose is delivered at a higher dose-rate and a reduction of cell repair is expected, resulting in an increased RE. As a result, the RE function is more sensitive to variation in the short half-time region. The maximal RE is obtained when both half-times tend to zero. This special situation corresponds to a single acute dose delivery, i.e., a factor $G_{2,1}$ of 1. RE factors associated to red marrow are rather close to 1 as shown in Fig. 1. Considering effective half-times in blood above 20 h, the RE is less than 1.02 for the four isotopes of interest. Therefore, for radioimmunotherapy, since radiolabeled antibodies such as ^{131}I-tositumomab and ^{90}Y-ibritumomab tiuxetan tend to clear slowly, the BED is approximately equal to the absorbed dose. For PRRT, wash-out periods of peptides are usually short and effective clearance half-times in blood of about 1 h are appropriate. In this case, the RE factor ranges around 1.10. If an α/β ratio of 15 Gy is assumed instead of 10 Gy, the RE factors are smaller as illustrated in Fig. 2 by the shift of the isocurves in the direction of the shorter half-times. A similar pattern is observed when the repair half-time T_μ is shortened from 1.5 to 0.5 h [see Fig. 2(b)]. For radioiodine (^{131}I) therapy with rhTSH, clearance half-times from blood may be of the order of a few hours and RE factors are thus similar to those obtained from PRRT. A more complete estimate of the RE could be achieved using a biexponential function to describe clearance kinetics in blood. Irrespective of LQ model parameters, biological processes involving dose-rate and repair of sublethal damage, quantified by the RE, do not yield a BED to red marrow that is significantly different from the physical absorbed dose, which is typically associated with uncertainties of more than 20%. This is in contrast to results in murine models suggesting a strong in-fluence of the dose-rate on the resulting myelotoxicity.[21] Action involving stem cell repopulation and dose-rate may be responsible for these observations. Indeed, unlike normal organs with late response to radiation, such as kidneys, red marrow is an acute-responding tissue where significant cell repopulation occurs during irradiation. Based on the LQ model accounting for cell repopulation, the BED has been extended by Dale[28] as follows: BED=D·RE–BRF. The BED related repopulation factor BRF is expressed in the form of a dose that reduces the biological effect due to concurrent cell repopulation. Using this model, Howell *et al.*[29] examined the advantage of longer-lived radionuclides in radioimmunotherapy. Wilder *et al.*[10] studied the correlation between the BED including cell repopulation and hematopoietic toxicity after ^{131}I-Lym-1 infusions in patients.

No clear association between bone marrow absorbed dose or BED was found. As expected, the RE had only a minor effect upon BED. They suggested that the weak association had been influenced by tumor involvement of the red marrow or previous myelotoxic therapy. A BED formula including cell repopulation dedicated to radionuclide therapy has been derived by Atthey *et al.* in case of a single exponentially decaying source.[30] The formulation becomes more complex when the dose-rate temporal pattern depends on multiple irradiating source organs and no analytical solution has been found in this case. It should be noted that the bone marrow is a highly complex organ and other factors that may influence dose response, such as spatial distribution of active bone marrow and hematopoietic cells, remain outside the scope of the present study.[31]

In the case of kidneys, the RE factors take higher values than in the case of red marrow. For effective clearance half-times between 10 and 60 h, the RE to the renal cortex ranges between 1.5 and 4. Figure 3 shows that the medulla half-time contributes more significantly to the cortex RE as the ratio $S_{\text{cort}\leftarrow\text{cort}}/S_{\text{cort}\leftarrow\text{med}}$ decreases across the different radionuclides examined. For a low-energy beta emitter such as ^{177}Lu, the RE function is almost insensitive to $T_{1/2,\text{med}}$ variations and the resulting isocurves are nearly straight lines parallel to the $T_{1/2,\text{med}}$ axis. The highest medulla contribution is obtained for ^{111}In due to the small $S_{\text{cort}\leftarrow\text{cort}}/S_{\text{cort}\leftarrow\text{med}}$ ratio resulting from low electron dose deposition within the cortex from decays in the medulla. Figures 4(a) and 4(b) show that the RE isocurve pattern is strongly influenced by the initial intake fraction ratio. In fact, according to Eq. (9), initial intake factors contribute directly to the determination of the initial dose-rate that is critical for BED considerations. Figures 4(c) and 4(d) show that fractionation reduces the RE values and narrows the range of RE values as the number of cycles increases without affecting the shape of the functional dependence of $T_{1/2,\text{cort}}$ and $T_{1/2,\text{med}}$. One to five cycles are typical fractionated regimens in PRRT.

The scenario with $f_{\text{cort}}/f_{\text{med}}=3$, i.e., an initial radioactivity distribution of 3/4 in the cortex and 1/4 in the medulla, corresponds to a realistic situation in PRRT as shown by Konijnenberg *et al.*[32] According to Barone *et al.*,[1] the mean effective clearance half-time of ^{90}Y-DOTATOC in kidneys is about 30 h. In this case, Fig. 4(a) yields a RE of about 1.9 and variations due to the medulla contribution are minor. Furthermore, with some retention in the cortex, the clearance in the medulla is certainly faster than in the cortex and fluctuations due to medulla are even smaller. As long as the renal activity is essentially located in the cortex of the kidney, the medulla contribution may be neglected. Then it is reasonable to use Eq. (3) with a single source organ. In their study, Barone *et al.*[1] determined the BED to kidneys for each patient based on Eqs. (3) and (17). The results show a correlation between BED and renal toxicity, as opposed to the absorbed dose alone. This finding clearly demonstrates that BED is an appropriate quantity to improve prediction in dose-toxicity response. Those considerations suppose that the dose to the cortex is responsible for the radiation-induced renal diseases observed after radionuclide therapy. The irregular activity distribution within the cortex observed by de Jong *et al.*[23] limits the appropriateness of MIRD19 and ideally imposes the use of three-dimensional (3D) voxel-based dosimetry. Indeed, for low-energy β-emitters (such as ^{111}Lu) and Auger electron emitters (such as ^{111}In), Konijnenberg *et al.*[32] showed that heterogeneous activity distribution in the kidneys affects considerably the dose distribution, generating volumes with lower and higher doses than the average dose to the cortex. In contrast, for high-energy β- emitters (such as ^{90}Y), dose distributions in the kidneys are essentially independent of the activity distribution pattern and, consequently, accurate kidney dosimetry can be based on MIRD19. Furthermore, using the Lyman model with the effective volume method, Konijnenberg *et al.* interpreted the nonuniform dose distributions over the kidney irrespective of any heterogeneity in activity distributions and suggested that the EBRT tolerance dose to kidneys, i.e., 23 Gy, may be augmented at least by a factor of 1.25 for PRRT. With respect to effects and limitations of dose nonuniformity, the MIRD19-based BED dosimetry enables a suitable intermediate level between the rough whole kidney dosimetry and

the complex 3D voxel-based BED dosimetry. With current quantitative PET and SPECT imaging, activity uptake may be measured appropriately in the different renal regions.[33]

Figure 5 shows the largest safe dose to be delivered to the renal cortex according to effective clearance half-times in the cortex and medulla. As expected, fractionation of the total dose results in higher maximum tolerated doses, of about 30%–40% for a three-dose fractionation regimen, as compared to the unfractionated total dose. This type of approach is interesting for a first estimate of the maximal dose to an organ at risk in case of phase I/II trials of new therapeutic radiopharmaceuticals. At present, it is unclear which dose can be administered safely to kidneys in the context of radionuclide therapy.[34] For instance, in skeletal targeted radiotherapy with ^{166}Ho-DOTMP, nephropathy was reported for low absorbed dose to kidneys below 4 Gy.[4] Since the radioisotope passes fast into the urine with minimal retention in the kidneys, the dose-rate effects have certainly accounted for the toxicity observed. However, the RE of 1.3 calculated by the authors using Eq. (3) does not provide a sufficient explanation and the renal toxicities observed in this study remain unclear. Recently, Chiesa *et al.*[5] used the single organ BED concept to determine the maximal activity to be administered to patients in the ongoing phase I escalation study of myeloablative ^{90}Y-ibritumomab tiuxetan therapy. BED toxicity thresholds were derived from EBRT for kidneys, but also heart, liver, lung, and testes. With myeloablative radionuclide therapy, accurate dosimetry of late-responding organs is essential for the design of the protocol in order to identify the second limiting organ(s) and then minimize or avoid toxicity.

Equations (1), (4), and (13) provide a generalized MIRD-based formalism to determine the BED in addition to absorbed dose. The implementation of the formulas in MIRD-based dosimetry software such as the OLINDA/EXM code[19] require minor modifications. Biokinetic parameters are directly available from conventional multiexponential fits. Thus, radiobiological parameters α/β and repair rate constants μ are the only "new" quantities necessary for the computation. However, large uncertainties associated with α/β and μ necessitate caution, particularly when the method is applied to an individual patient. Indeed, radiosensitivity may differ among patients and is probably influenced by prior therapy. In addition, LQ model parameters currently available have been derived from EBRT that produces homogeneous dose distribution whereas, in radionuclide therapy, the dose pattern depends on the targeting of the therapeutic agents, e.g., stem cells for bone marrow in RIT or glomeruli for renal cortex in PRRT. Therefore, α/β and μ should be determined specifically for each new radiotherapeutic agent. The MIRD formalism is not limited to uniform activity distribution in organs or suborgans but is also appropriate for voxel-based dosimetry.[35]Equation (13) is then directly applicable at the voxel level and completes the simplified formula proposed by Prideaux *et al.*[9] However, substantial computer time will be required for this task and appropriate algorithms for 3D imaging based BED dosimetry are still under investigation.

V. CONCLUSION

In addition to physical absorbed dose, the BED takes into account competing effects of dose-rate and tissue repair mechanism. In this work, a generic formula has been proposed to enlarge the BED formalism to the MIRD schema. The concern of dose-rate effect with cell repopulation that is relevant for acute-responding tissues such as red marrow and tumors requires more complex modeling and has not been considered in this study. It is generally admitted that BED may be a useful quantity to better predict dose-response and dose-toxicity relationships. Those relations are important in radionuclide therapy to optimize and evaluate treatment plans and modalities. Using radiation tolerance known from external radiation therapy, the BED formula may be used as a treatment-planning tool to incorporate dose-rate considerations when determining the activity to be administered. Although the LQ model is probably the best currently available model for radiation effect, large uncertainties are associated with

radiobiological parameters, such as α/β or μ, that are crucial for BED calculation. Nevertheless, useful guidance could be obtained if those uncertainties are considered as an inherent part of treatment planning and clinical decision-making process.

The BED-based dosimetry was applied to the red marrow as well as the regional kidney model considering the cortex and the medulla. Red marrow dosimetry is of interest since hematopoietic suppression is the dose-limiting toxicity for most nonmyeolablative therapies. It has been shown that the dose-rate associated with repair mechanism does not play a major role for red marrow. With the increasing use of small radiolabeled molecules such as peptides, assessing the impact of the dose-rate in kidney dosimetry is of clinical significance due to the rapid excretion through the urinary tract and the retention of radioactivity in the renal cortex. In this case, the BED may differ largely from the absorbed dose and complex relations occur between biokinetic and dose parameters of both the cortex and the medulla.

Acknowledgments

The present study is supported by the Swiss National Science Foundation (Fellowship No. PBFR2-115886) and NIH/NCI Grant No. R01 CA116477.

References

1. Barone R, Borson-Chazot FO, Valkerna R, Walrand S, Chauvin F, Gogou L, Kvols LK, Krenning EP, Jamar F, Pauwels S. Patient-specific dosimetry in predicting renal toxicity with Y-90-DOTATOC: Relevance of kidney volume and dose-rate in finding a dose-effect relationship. J Nucl Med 2005;46:99S–106S. [PubMed: 15653658]
2. Behr TM, Memtsoudis S, Sharkey RM, Blumenthal RD, Dunn RM, Gratz S, Wieland E, Nebendahl K, Schmidberger H, Goldenberg DM, Becker W. Experimental studies on the role of antibody fragments in cancer radioimmunotherapy: Influence of radiation dose and dose-rate on toxicity and anti-tumor efficacy. Int J Cancer 1998;77:787–795. [PubMed: 9688314]
3. Bodey RK, Evans PM, Flux GD. Application of the linear-quadratic model to combined modality radiotherapy. Int J Radiat Oncol Biol Phys 2004;59:228–241. [PubMed: 15093920]
4. Breitz HB, Wendt RE III, Stabin MS, Shen S, Erwin WD, Rajendran JG, Eary JF, Durack L, Delpassand E, Martin W, Meredith RF. 166Ho-DOTMP radiation-absorbed dose estimation for skeletal targeted radiotherapy. J Nucl Med 2006;47:534–542. [PubMed: 16513624]
5. Chiesa C, Botta F, Di Betta E, Coliva A, Maccauro M, Aliberti G, Bavusi S, Devizzi L, Guidetti A, Seregni E, Gianni AM, Bombardieri E. Dosimetry in myeloablative 90Y-labeled ibritumomab tiuxetan therapy: Possibility of increasing administered activity on the base of biological effective dose evaluation. Preliminary results. Cancer Biother Radiopharm 2007;22:113–120. [PubMed: 17627419]
6. Dale RG. Dose-rate effects in targeted radiotherapy. Phys Med Biol 1996;41:1871–1884. [PubMed: 8912367]
7. Howell RW, Goddu SM, Rao DV. Application of the linear-quadratic model to radioimmunotherapy: Further support for the advantage of longer-lived radionuclides. J Nucl Med 1994;35:1861–1869. [PubMed: 7965170]
8. Konijnenberg MW. Is the renal dosimetry for [90Y-DOTA0,Tyr3]octreotide accurate enough to predict thresholds for individual patients? Cancer Biother Radiopharm 2003;18:619–625. [PubMed: 14503958]
9. Prideaux AR, Song H, Hobbs RF, He B, Frey EC, Ladenson PW, Wahl RL, Sgouros G. Three-dimensional radiobiologic dosimetry: Application of radiobiologic modeling to patient-specific 3-dimensional imaging-based internal dosimetry. J Nucl Med 2007;48:1008–1016. [PubMed: 17504874]
10. Wilder RB, DeNardo GL, Sheri S, Fowler JF, Wessels BW, DeNardo SJ. Application of the linear-quadratic model to myelotoxicity associated with radioimmunotherapy. Eur J Nucl Med 1996;23:953–957. [PubMed: 8753685]

11. Dale RG. The application of the linear-quadratic dose-effect equation to fractionated and protracted radiotherapy. Br J Radiol 1985;58:515–528. [PubMed: 4063711]
12. Fowler JF. The linear-quadratic formula and progress in fractionated radiotherapy. Br J Radiol 1989;62:679–694. [PubMed: 2670032]
13. Loevinger, R.; Budinger, TF.; Watson, EE. MIRD Primer for Absorbed Dose Calculations. The Society of Nuclear Medicine, Inc; New York: 1991. revised edition
14. Joiner, MC.; van der Kogel, AJ. Basic Clinical Radiobiology. 3. Steel, GG., editor. Arnold; London: 2002.
15. Dale R, Carabe-Fernandez A. The radiobiology of conventional radiotherapy and its application to radionuclide therapy. Cancer Biother Radiopharm 2005;20:47–51. [PubMed: 15778580]
16. Millar WT. Application of the linear-quadratic model with incomplete repair to radionuclide directed therapy. Br J Radiol 1991;64:242–251. [PubMed: 2021798]
17. Brenner DJ, Hlatky LR, Hahnfeldt PJ, Huang Y, Sachs RK. The linear-quadratic model and most other common radiobiological models result in similar predictions of time-dose relationships. Radiat Res 1998;150:83–91. [PubMed: 9650605]
18. Dale RG. A graphical method to simplify the application of the linear-quadratic dose-effect equation to fractionated radiotherapy. Br J Radiol 1986;59:1111–1115. [PubMed: 3790899]
19. Stabin MG, Sparks RB, Crowe E. OLINDA/EXM: The second-generation personal computer software for internal dose assessment in nuclear medicine. J Nucl Med 2005;46:1023–1027. [PubMed: 15937315]
20. Sgouros G. Bone marrow dosimetry for radioimmunotherapy: Theoretical considerations. J Nucl Med 1993;34:689–694. [PubMed: 8455089]
21. Behr TM, Behe M, Sgouros G. Correlation of red marrow radiation dosimetry with myelotoxicity: Empirical factors influencing the radiation-induced myelotoxicity of radiolabeled antibodies, fragments and peptides in pre-clinical and clinical settings. Cancer Biother Radiopharm 2002;17:445–464. [PubMed: 12396708]
22. O'Donoghue JA, Baidoo N, Deland D, Welt S, Divgi CR, Sgouros G. Hematologic toxicity in radioimmunotherapy: Dose-response relationships for I-131 labeled antibody therapy. Cancer Biother Radiopharm 2002;17:435–443. [PubMed: 12396707]
23. De Jong M, Valkema R, van Gameren A, Van Boven H, Bex A, Van De Weyer EP, Burggraaf JD, Korner M, Reubi JC, Krenning EP. Inhomogeneous localization of radioactivity in the human kidney after injection of [(111)In-DTPA]octreotide. J Nucl Med 2004;45:1168–1171. [PubMed: 15235063]
24. Lambert B, Cybulla M, Weiner SM, Van De Wiele C, Ham H, Dierckx RA, Otte A. Renal toxicity after radionuclide therapy. Radiat Res 2004;161:607–611. [PubMed: 15161361]
25. Flynn AA, Pedley RB, Green AJ, Dearling JL, El Emir E, Boxer GM, Boden R, Begent RH. The nonuniformity of antibody distribution in the kidney and its influence on dosimetry. Radiat Res 2003;159:182–189. [PubMed: 12537523]
26. Bouchet LG, Bolch WE, Blanco HP, Wessels BW, Siegel JA, Rajon DA, Clairand I, Sgouros G. MIRD Pamphlet No 19: Absorbed fractions and radionuclide S values for six age-dependent multi-region models of the kidney. J Nucl Med 2003;44:1113–1147. [PubMed: 12843230]
27. Emami B, Lyman J, Brown A, Coia L, Goitein M, Munzenrider JE, Shank B, Solin LJ, Wesson M. Tolerance of normal tissue to therapeutic irradiation. Int J Radiat Oncol Biol Phys 1991;21:109–122. [PubMed: 2032882]
28. Dale RG. Radiobiological assessment of permanent implants using tumour repopulation factors in the linear-quadratic model. Br J Radiol 1989;62:241–244. [PubMed: 2702381]
29. Howell RW, Goddu SM, Rao DV. Proliferation and the advantage of longer-lived radionuclides in radioimmunotherapy. Med Phys 1998;25:37–42. [PubMed: 9472824]
30. Atthey M, Nahum AE, Flower MA, McCready VR. Effects of cellular repair and proliferation on targeted radionuclide therapy: A modelling study. Phys Med Biol 2000;45:N15–N20. [PubMed: 10795994]
31. Watchman CJ, Bourke VA, Lyon JR, Knowlton AE, Butler SL, Grier DD, Wingard JR, Braylan RC, Bolch WE. Spatial distribution of blood vessels and CD34+ hematopoietic stem and progenitor cells within the marrow cavities of human cancellous bone. J Nucl Med 2007;48:645–654. [PubMed: 17401104]

32. Konijnenberg M, Melis M, Valkema R, Krenning E, de Jong M. Radiation dose distribution in human kidneys by octreotides in peptide receptor radionuclide therapy. J Nucl Med 2007;48:134–142. [PubMed: 17204710]

33. Helisch A, Forster GJ, Reber H, Buchholz HG, Arnold R, Goke B, Weber MM, Wiedenmann B, Pauwels S, Haus U, Bouterfa H, Bartenstein P. Pre-therapeutic dosimetry and biodistribution of Y-86-DOTA-Phe(1)-Tyr(3)-octreotide versus In-111-pentetreotide in patients with advanced neuroendocrine tumours. Eur J Nucl Med Mol Imaging 2004;31:1386–1392. [PubMed: 15175836]

34. O'Donoghue J. Relevance of external beam dose-response relationships to kidney toxicity associated with radionuclide therapy. Cancer Biother Radiopharm 2004;19:378–387. [PubMed: 15285886]

35. Bolch WE, Bouchet LG, Robertson JS, Wessels BW, Siegel JA, Howell RW, Erdi AK, Aydogan B, Costes S, Watson EE, Brill AB, Charkes ND, Fisher DR, Hays MT, Thomas SR. MIRD Pamphlet No. 17: The dosimetry of nonuniform activity distributions–radionuclide S values at the voxel level. Medical Internal Radiation Dose Committee. J Nucl Med 1999;40:11S–36S. [PubMed: 9935083]

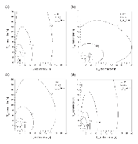

Fig. 1.
Relative effectiveness isocurves of the red marrow for (a) ^{90}Y, (b) ^{111}In, (c) ^{131}I, and (d) ^{177}Lu as a function of effective clearance half-times ($T_{1/2,b}$ and $T_{1/2,\mathrm{RB}}$) assuming an initial intake ratio $f_{\mathrm{RM}}/f_{\mathrm{RB}}$ of 0.05.

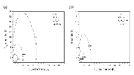

Fig. 2.
Relative effectiveness isocurves of the red marrow for ^{90}Y as a function of effective clearance half-times ($T_{1/2,b}$ and $T_{1/2,\mathrm{RB}}$) assuming $f_{\mathrm{RM}}/f_{\mathrm{RB}}$ =0.05 and (a) a different α/β =15 Gy and (b) a different T_{μ} =0.5 h.

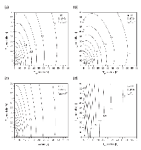

Fig. 3.
Relative effectiveness isocurves of the renal cortex for (a) ^{90}Y, (b) ^{111}In, (c) ^{131}I, and (d) ^{177}Lu as a function of effective clearance half-times ($T_{1/2,cort}$ and $T_{1/2,med}$) assuming an initial intake ratio f_{cort}/f_{med} of 1.

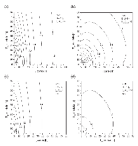

Fig. 4.
Relative effectiveness isocurves of the renal cortex for ^{90}Y as a function of effective clearance half-times ($T_{1/2,cort}$ and $T_{1/2,med}$) assuming an initial intake ratio f_{cort}/f_{med} of respectively, 3 (a), (c) and 1/3 (b), (d). A fractionated regimen was also considered with (c) N =2 cycles and (d) N =4 cycles.

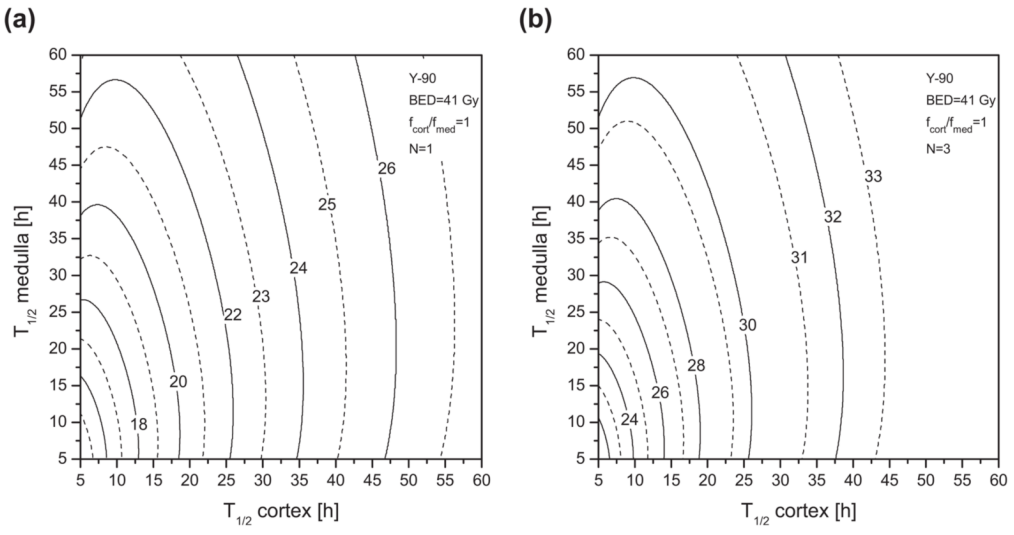

Fig. 5.

Isocurves of the largest safe absorbed dose to the renal cortex (in Gy) as a function of effective clearance half-times ($T_{1/2,cort}$ and $T_{1/2,med}$)assuming a BED of 41 Gy and an initial intake ratio f_{cort}/f_{med}=1 for ^{90}Y. A fractionated regimen was considered in (b) with N=3 cycles.

Table I

S values for the red marrow as target tissue for the common radionuclides in radionuclide therapy (Ref. [19]).

Isotopes	$S_{RM \leftarrow RM}$ (mGy/MBq s)	$S_{RM \leftarrow TB}$ (mGy/MBq s)	$S_{RM \leftarrow RB}$ (mGy/MBq s)	$S_{RM \leftarrow RM}/S_{RM \leftarrow RB}$
Y-90	5.87×10^{-5}	1.41×10^{-6}	5.26×10^{-7}	112
In-111	4.31×10^{-6}	4.04×10^{-7}	3.44×10^{-7}	12.5
I-131	1.55×10^{-5}	6.29×10^{-7}	4.00×10^{-7}	38.8
Lu-177	1.19×10^{-5}	2.67×10^{-7}	8.75×10^{-8}	136

Table II

S values for the renal cortex as target tissue for the common radionuclides in radionuclide therapy (Ref. [26]).

Isotopes	$S_{cort \leftarrow cort}$ (mGy/MBq s)	$S_{cort \leftarrow med}$ (mGy/MBq s)	$S_{cort \leftarrow cort}/S_{cort \leftarrow med}$
Y-90	6.28×10^{-4}	1.13×10^{-4}	5.6
In-111	4.70×10^{-5}	1.59×10^{-5}	3.0
I-131	1.64×10^{-4}	1.53×10^{-5}	10.7
Lu-177	1.17×10^{-4}	2.62×10^{-6}	44.7